NRL Report 6766

Attenuation of Microwave Radiation for Paths Through the Atmosphere

R. A. LeFande

Satellite Communication Branch
Radio Division

November 29, 1968

NAVAL RESEARCH LABORATORY
Washington, D.C.

CONTENTS

ABSTRACT

Microwave radiation is absorbed by atmospheric oxygen and water vapor and is absorbed and scattered by rainfall. This report provides values of these losses in the frequency decade from 10 to 100 GHz for paths through the atmosphere at elevation angles from 0 to 90 degrees.

The theoretical expressions for oxygen absorption are assembled in explicit form. The resonant frequencies are taken from published low-pressure measurements, and the entire absorption profile is fitted to published intermediate and atmospheric pressure results, with a constant of proportionality and the absorption resonance line width used as fitting parameters. The absorption line breadth is found to deviate from the accepted linear pressure dependence, increasing approximately as the square root of pressure for pressures above one-half atmospheric.

The results of similar analyses of water vapor absorption are assembled and combined with the results of oxygen absorption analyses to obtain the complete absorption coefficients as a function of the atmospheric parameters.

The total attenuation due to absorption in the clear atmosphere is computed for a model atmosphere with various water vapor concentrations. Results are provided in graphical form, giving attenuation as a function of frequency and elevation angle.

The prediction of rainfall attenuation is severely limited by the absence of meaningful statistics on rain rate and storm structure. Rough estimates for rain attenuation are made for crude model storms which occur for 1, 0.1, and 0.01 percent of the time. Total values of the attenuation for the model storms and the atmospheric absorption are provided.

PROBLEM STATUS

This is an interim report on one phase of the problems; work on other phases is continuing.

AUTHORIZATION

NRL Problems R01-34 and R01-36
Projects RF 14-222-41-4353 and XF 019-0204-11648

Manuscript submitted July 1, 1968.

ATTENUATION OF MICROWAVE RADIATION FOR PATHS THROUGH THE ATMOSPHERE

INTRODUCTION

The attenuation of microwave radiation in the frequency decade 10 to 100 GHz for propagation paths through the atmosphere at all elevation angles is of great interest in the analysis of experiments in radio astronomy and communications by satellite. The purpose of this report is to assemble the explicit theoretical expressions and measured constants used to compute the attenuation and to provide the results of such a calculation for a typical model atmosphere. The computation of attenuation for paths through the atmosphere requires a knowledge of the magnitude of the absorption by the atmospheric constituents, the frequency dependence, and the spatial variation of the effect along the path. The attenuation, in general, consists of two contributions that require quite different treatments. The first contribution is the absorption by the molecular oxygen and water vapor that controls the attenuation in the clear atmosphere and can be computed accurately. The second contribution is attenuation due to rainfall; this can be treated only qualitatively, but it is quite important to the communicator who is not always able to choose ideal conditions.

Molecular oxygen and water vapor absorption resonances or lines completely dominate the absorption spectrum in the band from 10 to 100 GHz. A review of the existing theoretical treatments and experimental measurements is made here to obtain expressions giving the coefficient of absorption as a function of frequency, temperature, and pressure. The total attenuation for paths of varying elevation angles is obtained for a model atmosphere by integrating the semiempirical expressions along the path.

First, the theoretical analyses are used to obtain the general expression describing the interaction of the incident radiation with the oxygen molecule. Then the various terms in the expression are identified and reduced to the form to be used in the path computations. In its final form, the expression determines the functional dependence of the absorption spectrum except for a function describing the shape of the resonances in the frequency domain and a constant.

The expression obtained for oxygen is adapted to the essentially similar water vapor interaction, and a semiempirical approximation of the contribution of resonances that occur beyond 100 GHz is introduced. The problem of obtaining a function to describe the shape of the resonance line is discussed, introducing additional pressure and temperature dependence and another fitting parameter, the line breadth.

The constants which remain in the theoretical functions are obtained by fitting published experimental data. Evidence for a pressure dependence for the oxygen line breadth different from the theoretical result is also derived from the data. The total attenuation due to absorption by oxygen and water vapor is computed as a function of frequency and elevation angle for the model atmosphere.

The attenuation due to rainfall is considered in an approximate manner in the last part of this report. The theoretical values of the attenuation as a function of frequency and rain rate are taken from published results. The severe limitations of the existing statistical data on the spatial and temporal distributions of rain rate are discussed, and some crude model storms are constructed. Finally, the attenuations produced by the

rain for propagation paths through the model storms are computed and combined with the attenuation due to oxygen and water vapor to obtain representative values of the total losses.

ABSORPTION BY MOLECULAR OXYGEN

The absorption of microwave energy by oxygen results from magnetic dipole interactions with the incident radiation due to the oxygen molecule's permanent magnetic dipole moment, which produces transitions between molecular fine structure levels of the allowed rotational states. A detailed discussion of the theory of microwave spectroscopy is beyond the scope of this report, and the various treatises (1-5) on which this work is based should be referred to for an exact exposition.

The actual amount of the incident radiation absorbed by a given transition in a gas of the molecules depends on the relative fraction (f_i) of the molecules which are in the lower energy state of the transition and on the square of the matrix element of the dipole moment connecting the two states. The magnitude of the matrix element is a measure of the effectiveness of the radiation in producing the transition.

The complete expression as obtained by Van Vleck (4) for the absorption coefficient γ of a gas of molecules having a series of transitions has the form

$$\gamma = (\text{constant})\ \nu N \sum_{i,j} \left[|\mu_{j,i}|^2 f_j S(\nu_{j,i}, \nu) + |\mu_{i,j}|^2 f_i S(\nu_{i,j}, \nu) \right]$$

This expression consists of pairs of terms representing emission and absorption transitions between two states. The algebraic sum of the two terms is the net absorption and is dependent on the relative population of states of higher and lower energy. The subscripts i and j are labels representing states defined by a set of quantum numbers. The frequency of the incident radiation is ν, and $\nu_{j,i}$ is the resonant frequency of the absorption line. The resonant frequency is the frequency of the quanta of radiation energy equal to the difference between the energies of the initial and final states of the transition. N is the number of molecules per unit volume, $S(\nu_{j,i}, \nu)$ is a function describing the absorption line profile (i.e., the absorption versus frequency curve), $\mu_{i,j}$ is the matrix element connecting states i and j. The constant is a combination of physical and mathematical constants and is given by the exact theoretical treatments. As the predicted value does not fit the data perfectly, the constant will be used as a fitting parameter, and any physical constants subsequently introduced in this discussion will be absorbed into this term.

The energy level structure of the oxygen molecule with intervals in the microwave region is produced by interaction of the uncompensated electronic spin (total spin for molecule = 1) and the "end over end" rotational angular momentum of the molecule. The rotational levels (quantum number K) are split into levels corresponding to the allowable ways of constructing the total angular momentum vector. This level structure is modified further by the rotation of the molecule, the interaction between the processing component of the electron orbital angular momentum, and the total spin and centrifugal deformation of the molecule.

Symmetry considerations allow the rotational quantum number K to take on odd integral values 1, 3, ..., only. Corresponding to each K, two possible transitions, $J = K-1 \rightarrow J = K$ and $J = K \rightarrow J = K+1$ (J = total angular momentum quantum number), are allowed by the selection rules $\Delta J = \pm 1$, $\Delta K = 0$. The frequency of the quanta absorbed or emitted can then be calculated from the difference in the energy levels. The fine structure of oxygen results in an infinite series of lines grouped about 60 GHz, of which

approximately 25 can be detected in actual measurements. The energy levels have been computed by Schlapp (3) in fair detail, and Burkhalter et al. (6) have obtained the frequencies of 25 lines, which could be fitted to the Schlapp theory with the addition of empirical terms. The frequencies of additional lines too weak to measure can be obtained from such semiempirical fits.

The matrix elements are derived through quantum vector addition and obtain the form

$$|\mu_{K_+}|^2 = \frac{1}{3}\mu_0^2 \frac{K(2K+3)}{(2K+1)(K+1)},$$

$$|\mu_{K_-}|^2 = \frac{1}{3}\mu_0^2 \frac{(K+1)(2K-1)}{(2K+1)K},$$

$$|\mu_{K_0}|^2 = \frac{8}{3}\mu_0^2 \frac{(K^2+K+1)(2K+1)}{K(K+1)(2K+1)},$$

where μ_0 is the Bohr magneton. It should be noted that oxygen has lines at $\nu_{ij} = 0$ for each rotational level, which result in a nonresonant contribution to γ total. The subscripts K_- and K_+ denote the transitions $J = K-1 \rightarrow J = K$ and $J = K \rightarrow J = K+1$ respectively, while K_0 denotes the nonresonant term corresponding to that value of K.

The fraction of molecules in the jth state can be expressed as

$$f_j = (\text{w.f.})_j \frac{1}{Z} \exp(-E_j/kT),$$

$$Z = \sum_i (\text{w.f.})_i \exp(-E_i/kT),$$

a Boltzmann distribution with statistical weight factors (w.f.) reflecting the more frequent occurrence of certain states due to degeneracies. Z is the partition function, k is Boltzmann's constant, T the absolute temperature, and E_j the energy of the jth state, which depends in general on all of the quantum numbers defining the state.

In detailed treatments (see, for example, Ref. 2), f_j is expressed as $f_v(n) f_r(J,K,\psi)$, in which each term has the form given above; f_v is the fraction of states in a vibrational state defined by the principle quantum number n, and f_r the fraction of states which are in a rotational state defined by J, K, and ψ. For the oxygen molecule, the lowest vibrational frequency is sufficiently high that f_v is nearly 1 for the vibrational ground state at temperatures experienced in the atmosphere, and f_j can be considered equal to f_r.

If the identity $f_j - f_i = f_j(1 - f_i/f_j)$ is used, then the population difference is

$$f_j - f_i = f_j\left(1 - \frac{(\text{w.f.})_i e^{-E_i/kT}}{(\text{w.f.})_j e^{-E_j/kT}}\right).$$

For transitions between states of constant K,

$$(\text{w.f.})_i = (\text{w.f.})_j = 2K+1,$$

and

$$f_j - f_i = f_j\left[1 - e^{-(E_i - E_j)/kT}\right]$$

or

$$f_j - f_i = f_j\left[1 - e^{-h\nu_{ij}/kT}\right]$$

and since $h\nu_{ij} \ll kT$,

$$f_j - f_i \approx f_j \frac{h\nu_{ij}}{kT}$$

The dependence of γ on T obtained by Van Vleck (4) further assumes the energy E to depend on K only, and thus f_j has the approximate form

$$f_j \approx f_K = \frac{(2K+1)e^{-E_K/kT}}{\sum_l (2l+1)e^{-E_l/kT}}$$

where

$E_K = BK(K+1)$ and

$B = 2.862 \times 10^{-23}$ joule.

Since $|\mu_{ji}|^2 = |\mu_{ij}|^2$ and $S(\nu_{ji},\nu) = -S(\nu_{ij},\nu)$ (see Eq. (3)), γ can be written

$$\gamma = (\text{constant})\nu N \sum_{i,j} |\mu_{ij}|^2 S(\nu_{ij},\nu)(f_j - f_i) \quad ,$$

and γ becomes

$$\gamma = (\text{constant})\frac{\nu N}{T} \sum_{i,j} |\mu_{ij}|^2 \nu_{ij} S(\nu_{ij},\nu) f_j \tag{1}$$

If the atmosphere is assumed to be sufficiently dilute to be approximated by an ideal gas $N = P_{O_2}/kT$ where P_{O_2} is partial pressure of oxygen, so that

$$\gamma = (\text{constant})\frac{\nu P_{O_2}}{T^2} \sum_{i,j} |\mu_{ij}|^2 \nu_{ij} S(\nu_{ij},\nu) f_j$$

If the pressure dependence introduced through $S(\nu_{ij},\nu)$ is neglected for the moment, γ is directly proportional to partial pressure. At moderate temperatures, the energy levels are small compared to kT. $E \approx 0.05\ kT$, and the sum over all states in the denominator of f_j is approximately proportional to T. At frequencies removed from the resonant frequencies, the temperature dependence is given by T^{-2} because many lines contribute to the absorption so that the sum of the exponentials in the numerator tends to cancel that in the denominator (except for additional dependence introduced through $S(\nu_{ij},\nu)$). At frequencies where one line dominates, the dependence is given by

$$\frac{1}{T^3} \exp(-E_K/kT)$$

The form finally used in computing the absorption coefficients is

$$\gamma(\nu, T, P) = \nu_0 \left[\frac{P}{P_0}\right]\left[\frac{T_0}{T}\right]^2 \nu \left[\sum_{l\ \mathrm{odd}}^{51} (2l+1)\exp(-E_l/kT)\right]^{-1}$$

$$\cdot \sum_{K\ \mathrm{odd}}^{51} \left[\left(\frac{K(2K+3)}{K+1}\right)[\nu_{K_+} S(\nu_{K_+}, \nu)] + \frac{(K+1)(2K-1)}{K}[\nu_{K_-} S(\nu_{K_-}, \nu)]\right.$$

$$\left. + \frac{2(K^2+K+1)(2K+1)}{K(K+1)}\left\{\lim_{x\to 0}[x \cdot S(x, \nu)]\right\}\exp(-E_K/kT)\right] \qquad (2)$$

ν_0 is one of the constants adjusted in this work to give the best fit to the experimental data at P_0 and T_0, the ν_K are the frequency intervals or resonances of the spectrum, and

$$E_K/k = (2.0731)\,K(K+1)\ (^\circ\mathrm{K}) .$$

The summation is over odd values of K only and is cut off at $K = 51$, as the contribution of lines beyond this was found to be insignificant. The $\nu_{K_\pm}$ are taken from experimental results discussed in a later section for $K = 1$ to 25 and from the semiempirical models for $K = 25$ to 51:*

$$\nu_{K_-}(GHz) = 59.550 - 0.252K + 9.30\,K$$

$$\nu_{K_+}(GHz) = 59.790 + 0.252K - 9.30\,K$$

ABSORPTION BY WATER VAPOR

The absorption of microwave energy by water vapor (4,7) results from electric dipole interactions, and the theoretical treatment takes the same general form as that given for oxygen in the previous section.

The rotational level structure of water vapor is much more complex, consisting of a multitude of levels spaced at intervals in the microwave regions. Fortunately, the selection rules that result from the symmetry properties of the molecular levels permit only one transition in the frequency range of 10 to 100 GHz (at $\nu_0 = 22.254$ GHz), while several quite intense lines occur in the far infrared ($\nu > 100$ GHz). The absorption by water molecules then takes the form of one term of the sum of Eq. (1) above plus an additional semiempirical term approximating the total contribution of the low-frequency tails of the higher frequency lines. The fraction of molecules in the lth state, f_l, has the form $Z^{-1}\exp(-\ , kT)$, where Z is again the partition function which, for the case of water vapor, is a double sum over two quantum numbers with significant contributions from many states. By numerical evaluation, it can be shown that $Z \propto T^{-2}$ within a 10-percent error for variations of about 120°K in temperature (4).

The number density of water vapor molecules ν is proportional to the mass density . . The water vapor absorption can be expressed in terms of the vapor density . and

$$\cdot' = \nu_0' \cdot \left[\frac{T_0}{T}\right]\frac{1}{Z}[\exp(-E_0/kT)]\,\nu\,\nu_0 S(\ , \nu_0) .$$

where ν_0' is one of the constants adjusted to fit the experimental results.

*Adapted from the wave number result given in Table 1 of Ref. 4.

The residual absorption of higher frequency lines is given by a sum over the lines with $\nu_{ij} S(\nu_{ij}, \nu)$ replaced by its limit at $\nu_{ij} \gg \nu$. The exact calculation of this term is unprofitable, as the result is found to be only one-fourth of the observed residual absorption, probably due to the inadequacy of the theory of $S(\nu_{ij}, \nu)$ in this limit. The semiempirical result of Van Vleck (5) adequately describes the experimental results and will be used for the present purpose:

$$\alpha_{res} = (\text{constant}) \cdot \left(\frac{T_0}{T}\right) \nu \left[\lim_{\nu_{ij} \gg \nu} S(\nu_{ij}, \nu)\right]$$

ABSORPTION LINE SHAPE FUNCTION

The frequency dependence of the absorption coefficients obtained as discussed previously is largely determined by the line shape function $S(\nu_{ij}, \nu)$. The natural widths of the absorption resonances are very small ($\approx 10^{-5}$ Hz), resulting only from the growth of the amplitude of the vibrations upon absorption of the incident quanta. The observed line widths are of the order of 10^9 Hz at atmospheric pressure, and the absorption at frequencies removed from the resonant frequencies is completely controlled by this line broadening.

In the case of atmospheric gases, the lines are broadened by collisions between the molecules. Van Vleck and Weisskopf (8) have treated this classically by assuming the collisions to be sufficiently strong that the oscillator is stopped at the moment of collision and later restarted, with its phase with respect to the incident field determined by the condition that thermodynamic equilibrium exists between the ensemble of oscillators and the field. This requires that the time of the collision is much less than the mean time between collisions. The kinetic theory is applied to obtain the probability of occurrence for collisions. The results are combined and averaged over all the molecules to obtain the susceptibility and thereby the imaginary part of the index of refraction, the absorption coefficient.

Their result, known as the Van Vleck-Weisskopf shape factor, is

$$S(\nu_{ij}, \nu) = \frac{\nu}{\nu_{ij}} \frac{1}{\Delta\nu} \left[\frac{1}{\left(\frac{\nu - \nu_{ij}}{\Delta\nu}\right)^2 + 1} + \frac{1}{\left(\frac{\nu + \nu_{ij}}{\Delta\nu}\right)^2 + 1}\right], \tag{3}$$

where $\Delta\nu$ is the line breadth factor $\Delta\nu = 1/2\pi\tau$ (τ is mean time between collisions), which can obtain values of the order of ν_{ij}.

The limit used to describe the nonresonant absorption of oxygen is

$$\lim_{\nu \to 0} [\nu S(\nu, \nu)] = \frac{2\nu\Delta\nu}{\nu^2 + \Delta\nu^2}.$$

The limit of $S(\nu_{ij}, \nu)$ used to describe the absorption of the submillimeter water vapor lines is

$$S(\nu_{ij}, \nu) \xrightarrow[\nu_{ij} > \nu]{} (\text{constant}) \nu\Delta\nu.$$

Others have treated the problem using the methods of quantum mechanics and have obtained the same result when the same assumptions were made. There is, however, some question as to the validity of the simple assumption of strong collisions, and many

of the possible intermolecular forces, some acting at relatively long range, may affect the profiles of the absorption lines. In experimental determinations of $\Delta\nu$, it is in general difficult to fit the entire profile with this line shape function for a single value of $\Delta\nu$; for example, if $\Delta\nu$ is chosen to fit the region contiguous to the peak, the theoretical expression does not fit the tail.

Since the available empirical values of actual atmospheric absorption can be fitted to within their uncertainties by appropriate adjustment of the constants, the Van Vleck-Weisskopf line shape is usable in the present effort as a good model even though the theoretical treatment may not be completely satisfying.

The line breadth factor depends on the total number of molecules per unit volume N, their velocity v, and the cross section for collision σ: $\Delta\nu = Nv\sigma$. The collision cross section can be shown to be proportional to $v^{-2/(n-1)}$, where n is the exponent of the intermolecular force law ($F \propto r^{-n}$) and can assume values from 1 to 7. From kinetic theory, v is proportional to $T^{1/2}$, and from the ideal gas law $N \propto P/T$, so that

$$\Delta\nu \propto PT^{-\frac{n+1}{2(n-1)}}$$

Or, if $(\Delta\nu)_0$ is the line breadth measured at P_0, T_0, then

$$\Delta\nu = (\Delta\nu)_0 \left[\frac{P}{P_0}\right] \left[\frac{T}{T_0}\right]^{-x}$$

where x, the exponent of the temperature dependence at constant pressure, is

$$x = \frac{n+1}{2(n-1)}$$

The simple linear pressure dependence of $\Delta\nu$ is tested on experimental data in the next section and is found to hold only at lower pressures. Apparently at pressures of 300 mm Hg and higher, the individual collisions become less effective in broadening the line (possibly due to either an increasing number of multiple molecular collisions or the failure of a molecule to regain equilibrium between collisions), with the result that measurements in the range of 300 to 760 mm Hg appear to exhibit an approximately $P^{1/2}$ dependence.

The pressure and temperature dependence of the line breadth factor enters into the complete expression for the absorption coefficient (Eq. (2)) through $S(\ldots, T, P)$, contributing a further difference in the pressure and temperature variation of $\alpha(\nu, T, P)$ between that at frequencies adjacent to the resonant peaks and that at frequencies removed from the peaks. This simple behavior of the line breadth is further complicated by the dependence of the perturbing effect of the collisions on N. Measurements on individual lines at low pressures show that the variation of effective width from line to line is less than 10 percent of the width, so that using an average value weighted over line strength results in a small error (9).

DETERMINATION OF CONSTANTS BASED ON PUBLISHED EXPERIMENTAL DATA

Oxygen

The experiments that have been conducted are of two general types: measurements of γ, the ν_{A_0} or $\Delta\nu$ at reduced pressure and measurement of the actual effect of the

absorption at atmospheric pressure on a signal — either in the laboratory or over a typical path through the atmosphere.

The determination of the frequency intervals of the absorption lines must be obtained in a laboratory experiment at low pressure so that the individual lines can be separated. Determinations for $K = 1$ to 25 by three investigators are listed in Table 1. The results of the three measurements can be considered the same for the present purpose, and Burkhalter's (6) more complete results will be used in the computation of the attenuation.

The experimental determination of the constant ν_0 and the line breadth has been taken in two ways: by direct measurement of each individual line profile at low pressure and by use of $\Delta\nu$ as a parameter to obtain the best theoretical fit to the measured absorption profiles at atmospheric pressure.

The results obtained for the line breadth at low pressure are consistently about 1.5 GHz/atm with consistent linear pressure dependence, while field measurements at

Table 1
Experimental Determinations of Absorption Line Frequency Intervals and Line Breadths

Series (K_z)	Absorption Line Frequencies, ν_{K_z} (GHz)			Line Breadth Factors at Unit Pressure, $\Delta\nu/P$ (GHz/atm)			
	Burkhalter (6)	Mizusuhima (1)	Gokhale (10)	Artman (11)	Burkhalter (6)	Gokhale (10)	Anderson (9)
25-	53.5922	53.5994	—	—	—	—	—
23-	54.1300	54.1294	—	—	—	—	1.13
21-	54.6725	—	—	—	0.63	—	0.96
19-	55.2208	55.2216	—	1.46	—	—	1.23
17-	55.7841	55.7846	—	1.38	—	—	1.34
1+	56.2651	56.2656	56.2656	1.67	—	1.05	1.49
15-	56.3628	56.3640	56.3642	1.51	—	1.44	—
13-	56.9687	56.9708	—	1.41	—	—	1.42
11-	57.6120	57.6114	57.6123	1.50	—	1.02	—
9-	58.3240	58.3232	58.3249	1.52	—	0.63	1.50
3+	58.4462	58.4462	58.4463	1.69	—	0.84	1.30
7-	59.1634	59.1634	59.1642	1.38	—	0.84	—
5+	59.610	59.5914	—	1.49	—	—	—
5-	60.3064	60.3080	—	1.51	—	—	1.41
7+	60.436	60.4334	—	1.46	—	—	1.56
9+	61.120	61.1496	—	1.47	—	—	—
11+	61.8002	61.7998	—	—	—	—	1.50
13+	62.4117	62.4138	62.4129	—	0.66	0.75	—
3-	62.4861	62.4872	62.4862	—	1.59	1.11	1.46
15+	62.970	62.9966	—	—	—	—	1.35
17+	63.5683	63.5672	—	—	—	—	—
19+	64.1276	64.1280	—	—	—	—	1.20
21+	64.6789	64.6782	—	—	—	—	—
23+	65.220	65.2242	—	—	—	—	0.96
25+	65.770	—	—	—	—	—	—
1-	—	118.7505	—	—	—	—	—
Pressure (mm Hg)	≈ 1 mm	≈ 1	—	≈2 to 10	< 1	≈1 to 6	≈ 0 to 12

atmospheric pressure are consistently about 0.6 GHz/atm (12-15). The low-pressure individual line observations are also summarized in Table 1. This apparent inconsistency has been noted by others (4,16) and various theories have been suggested – notably that the effect of all the absorption lines is not a simple sum.

Artman and Gordon's data (11) at intermediate pressures provides a basis for determining $\cdot_{\cdot}$ and the actual pressure dependence of the line breadth factor.

Best-fit values for $\cdot_{\cdot}$ and $\cdot$ are obtained separately for sets of data points at 1, 0.5, and 0.25 atm pressure taken from Artman and Gordon's paper representing measurements of dry air. A least-squares-fit computer program is applied, assuming that the theoretical equations (Eqs. (2) and (3)) give at least the functional form of the profile correctly. The results* (for $T_{\cdot} = 300^{\circ}$K) are:

P (mm Hg)	$\cdot_0$ (dB/km GHz)	$\cdot P$ (GHz/atm)
760	0.01647 ± 0.00076	0.873 ± 0.195
380	0.01790 ± 0.00153	1.496 ± 0.456
180	0.01742 ± 0.00065	1.518 ± 0.200

Since $\cdot_{\cdot}$ should be constant, it can be fixed at its mean value = 0.0173 and the best-fit values of $\cdot P$ obtained:

P (mm Hg)	$\cdot_0$ (dB/km GHz)	$\cdot P$ (GHz/atm)
760	0.0173	1.0791 ± 0.0585
380	0.0173	1.2987 ± 0.1583
190	0.0173	1.4995 ± 0.1659

In each case the fit is of about the same precision, and without further data it will be assumed that $\cdot_{\cdot}$ is indeed constant.†

The choice of $\cdot$ is quite important, since the value largely determines the absorption at frequencies removed from the resonant peaks, which is the region of greatest interest for propagation purposes. The theory of the line broadening has been the subject of many studies, but none has yet predicted exactly the correct value or behavior with temperature and pressure so that it is necessary to use a semiempirical approach using the magnitude of $\cdot$ as a fitting parameter and a semiempirical model to give the pressure and temperature dependence. Since the use of $\cdot$ as a curve-fitting parameter becomes quite subjective when only a few data points are available as in some of the actual path loss measurements (13,15), the model for $\cdot(P,T)$ used in the present work is based on the study of Artman and Gordon's data. The adopted model is

*Iannuzzi (17) claims there is another related effect of the collision process in which the phase shifts induced by the collisions results in an effective displacement of the resonant frequencies with increasing pressure. He uses a pressure dependence of the form

$$\cdot_0 \quad \cdot_0 \; {}_{P=0} \; - \; \cdot P$$

to obtain a better fit to measurements obtained at pressures above 1 atm using a single line at $_0$ ~ 60 GHz to approximate the entire spectrum. In fitting Artman and Gordon's data, $\cdot$ was used as an additional parameter, allowing the resonant frequency of each resonance to be shifted by an amount proportional to the pressure. The mean value of $\cdot$ obtained for the six fits is -0.04 ± 0.27 MHz/mm. Without further evidence, this effect will be neglected for the present purpose and $\cdot$ will be set equal to zero.

†This value of $\cdot_0$ is greater than the theoretical value of $\cdot_0$ = 0.0145, which is obtained from the various constants and an assumed number fraction of oxygen (0.21).

$\Delta\nu = 0.00197\ \text{GHz}\ P(\text{mm Hg}), \qquad 0 < P \leq 350,$

$\Delta\nu = 0.690\ \text{GHz}\ [P(\text{mm Hg}) - 350]^{0.46}, \qquad P > 350.$

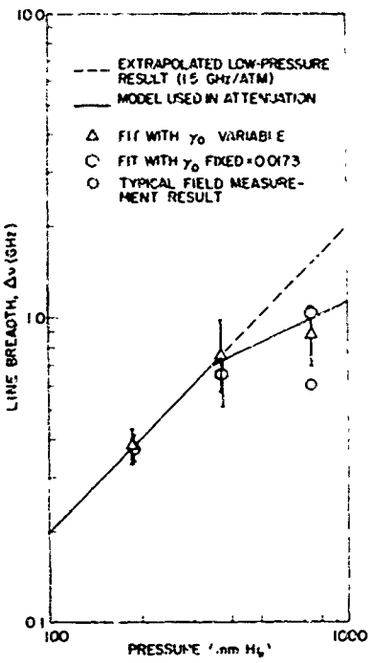

Fig. 1 - Line breadth vs pressure modeled to Artman and Gordon's (11) data

The values of $\Delta\nu(P)$ obtained in fitting Artman and Gordon's data and the resulting model of the pressure dependence of $\Delta\nu$ are plotted in Fig. 1. It is clear that $\Delta\nu$ begins to depart from a linear dependence on P for $P > 300$ mm Hg. The data points are plotted with the semiempirical curves that result from this model in Fig. 2.

The temperature dependence of $\Delta\nu$ at constant pressure has been measured by Tinkham and Strandberg (18) ($\gamma_{O_2} = 0.75$) and Beringer and Castle (19) ($\gamma_{O_2} = 0.87$). A mean value of $\gamma_{O_2} = 0.8$ will be used.

Water Vapor

Available measurements of water vapor absorption are less plentiful. The values of γ_0', E_0, and Z for the resonant water vapor absorption computed by Van Vleck (5) are found to satisfactorily describe the experimental data of Becker and Autler:

$$\frac{\gamma_0'}{f} = 0.1864\ \frac{\text{dB m}^3}{\text{km GHz g}}$$

$$\frac{E_0}{k} = 644\ ^\circ\text{K}$$

$$Z \approx 170 \left(\frac{T}{298}\right)^{3/2}$$

The line breadth parameter has been measured by Becker and Autler (20) and is found to depend on the water vapor density.

$$\Delta\nu = (\Delta\nu)_0 \frac{P}{P_0} (1 + 0.0046\rho)$$

at constant T. This vapor density dependence is an experimental result which reflects the greater effectiveness of H_2O–H_2O collisions in producing line broadening compared to H_2O-air collisions. The value of $(\Delta\nu)_0/P$ obtained at 318°K and small ρ is

$$\left.\frac{(\Delta\nu)_0}{P}\right|_{T=318^\circ\text{K}} = 2.61 \frac{\text{GHz}}{\text{atm}}$$

For the temperature dependence of $\Delta\nu$, the computed result of Benedict and Kaplan (21) will be used in the absence of experimental results: $n_{H_2O} = 0.63$.

The residual absorption of the submillimeter resonances is given by

$$\frac{\gamma_{res}'}{\rho} = (\gamma_{res}')_0 \left(\frac{T_0}{T}\right) \nu^2 \Delta\nu.$$

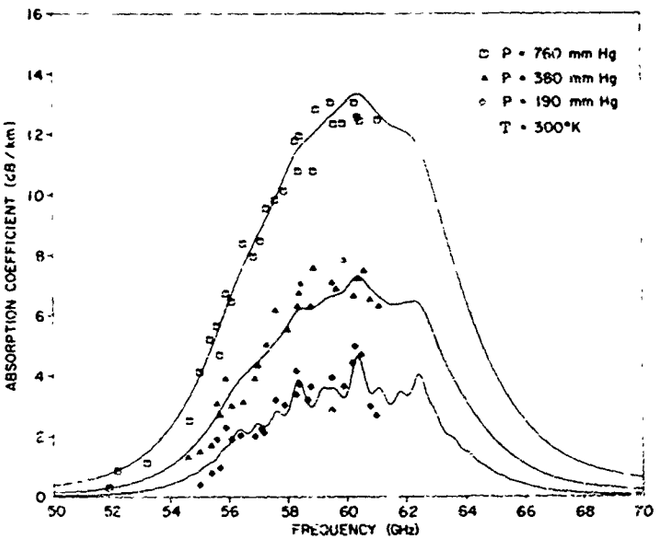

Fig. 2 - Artman and Gordon's data [11] with semi-empirical absorption curves, holding γ_0 constant (0.0173 dB/km GHz)

The value of $(\gamma'_{res})_0$ is found to increase with the water vapor density. Schulkin (22) has calculated $(\gamma'_{res})_0$ to fit Becker and Autler's data (20) using their result for the line breadth:

$$(\gamma'_{res})_0 = (1.85 + 0.02\rho) \times 10^{-6} \frac{\text{dB m}^3}{\text{km g GHz}^3}$$

The water vapor absorption curves are plotted with the oxygen curve in Fig. 3. The curves show that absorption by water vapor largely controls the total attenuation over the decade from 10 to 100 GHz except the region of high attenuation due to the oxygen resonances.

TOTAL ABSORPTION FOR PATHS THROUGH THE ATMOSPHERE

The absorption for a path through the atmosphere is given by

$$A(\infty, E)_{dB} = \int_0^\infty \gamma(T, P, \rho)\, dl ,$$

where l is the distance along the path measured from the ground, and T and P vary with altitude which in turn is a function of l and E, the elevation angle of the antenna.

The variation of temperature and pressure with altitude is not readily measured, so that a model is needed to represent typical or average conditions. The ARDC 1959 model atmosphere (23) is used for this purpose. A water vapor distribution proportional to a 10-year average distribution for the Washington, D.C., area (24) is also assumed. The

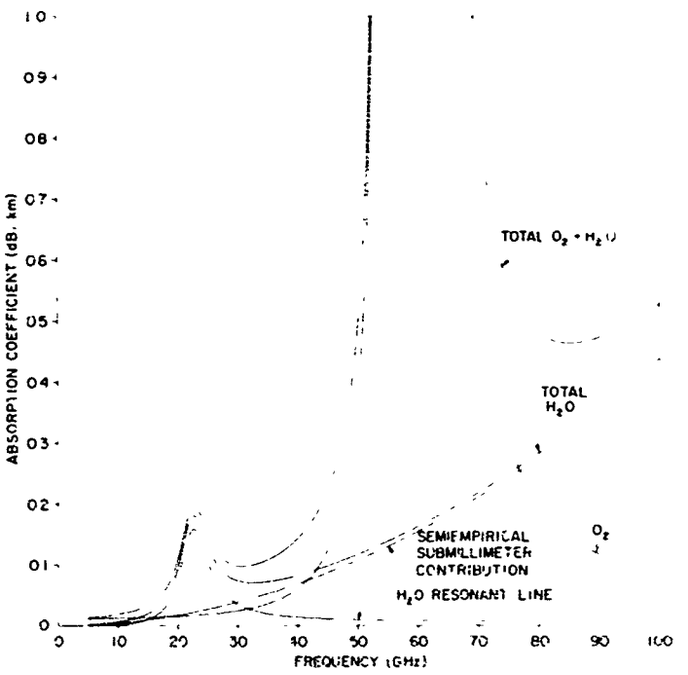

Fig. 3 - Water vapor and oxygen absorption coefficients vs frequency (T = 15°C = 60°F, P = 760 mm Hg, ρ_0 = 7.5 g/m^3)

ARDC profiles and the average water vapor distribution are shown in Fig. 4. The altitude dependence of the absorption coefficient (dB/km) that results from this model atmosphere is shown in Fig. 5. The curves plotted in Fig. 5 illustrate the difference in the dependence on altitude for frequencies close to the resonances of the absorption (e.g., 60 GHz) and those well removed from the resonances (e.g., 50 GHz). This difference is due to the cancellation of the pressure dependence of the absorption for frequencies exactly equal to that of the resonances. For these frequencies the absorption coefficient remains nearly constant to high altitudes, and for the nearby frequencies the decrease in the absorption is controlled only by the narrowing of the line breadth. The discontinuities that occur above ~ 12 km are due to the arbitrary cutoff in the assumed water vapor distribution.

The absorption profiles for various altitudes are three values of ground-level water vapor density (ρ_0), and are shown in Figs. 6 through 8. The chosen density values of 7.5, 15.0, and 22.5 g/m^3 correspond to 60-percent relative humidity at 60, 80, and 93°F, respectively. The curves show the rapid decrease with altitude of the absorption coefficient at frequencies away from the resonances and the nearly altitude-independent behavior at the oxygen peaks. Although the plotter does not have sufficient resolution to reproduce the full height of peaks at the resonances, the line structure of the oxygen absorption is in evidence at the highest altitude.

In the actual calculations applied here, the atmosphere is divided into a series of 110 spherical shells of exponentially increasing thickness to a height of 30 km.* Except

*Repeating the calculation with 110 layers from 0 to 30 km having uniform thicknesses produced essentially the same results.

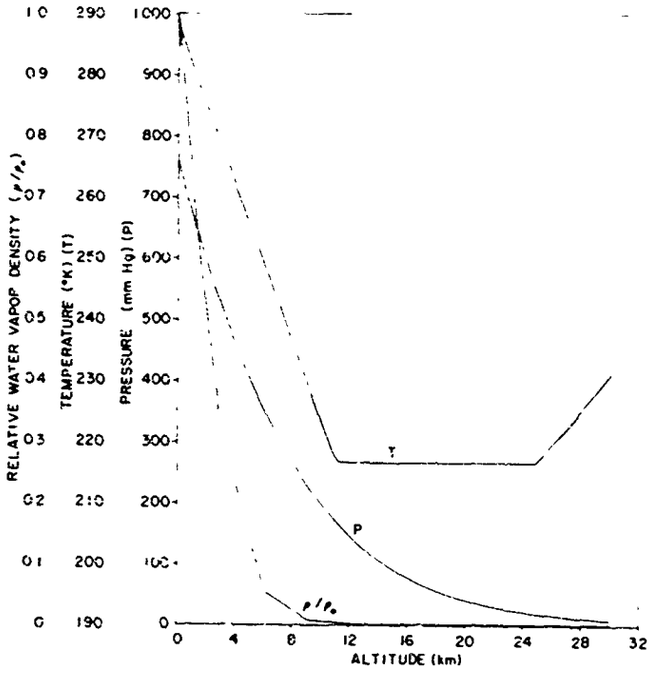

Fig. 4 - Temperature and pressure profiles of the 1959 ARDC model atmosphere, and average water vapor distribution

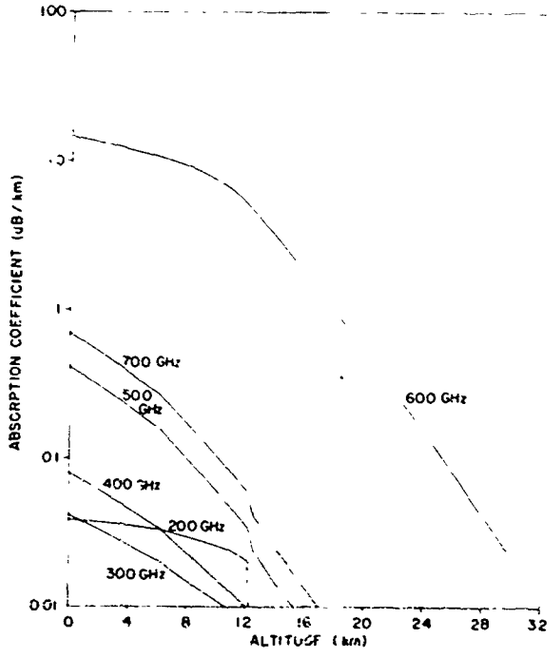

Fig. 5 - Net altitude dependence of absorption for the 1959 ARDC model atmosphere

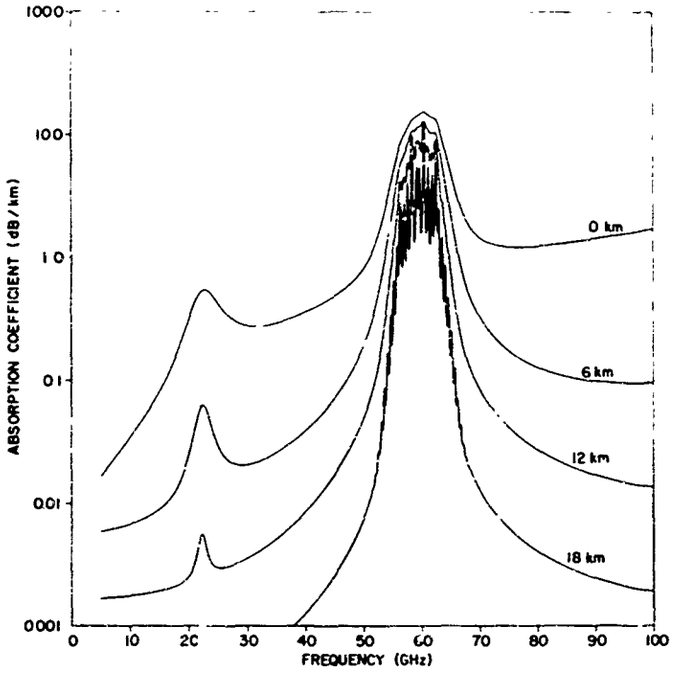

Fig. 6 - Absorption profiles for various altitudes for ρ_0 = 7.5 g/m^3 (60% RH at 60°F)

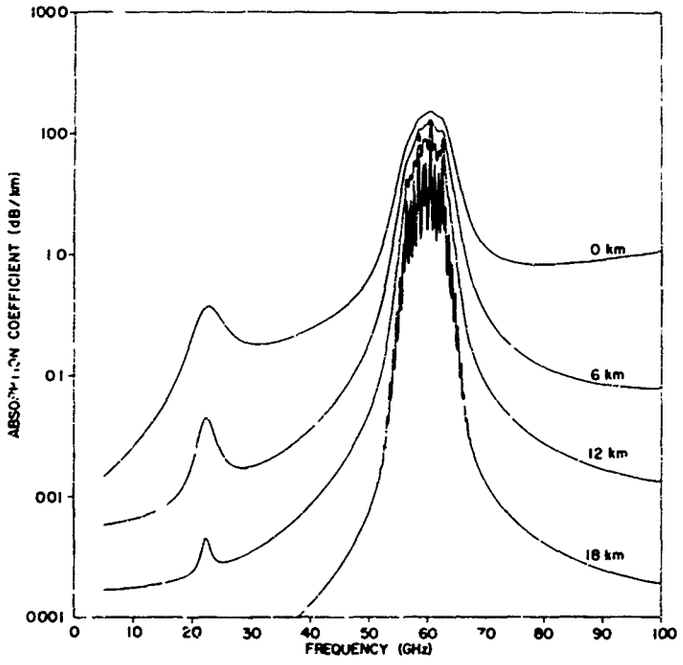

Fig. 7 - Absorption profiles for various altitudes for ρ_0 = 15.0 g/m^3 (60% RH at 80°F)

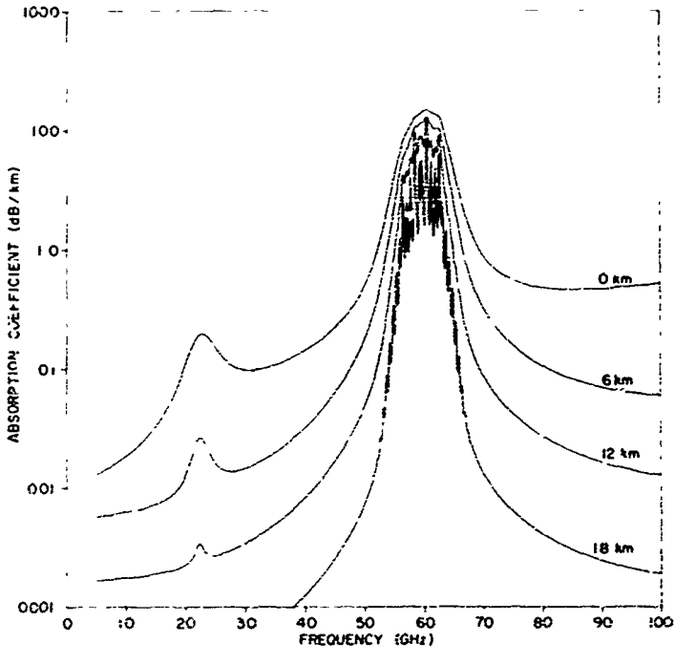

Fig. 8 - Absorption profiles for various altitudes for $\rho_0 = 22.5$ g/m^3 (60% RH at 93°F)

for single frequencies corresponding exactly to the resonances, the contribution of the attenuation from altitudes greater than 30 km is negligible.

The slant distance l_n thru the layer between the altitude h_n and altitude h_{n+1} is given by

$$l_n = a_e \left\{ \left[(H_n \sin E_n)^2 + (H_{n+1})^2 - (H_n)^2 \right]^{1/2} - H_n \sin E_n \right\} ,$$

where

$$H_n = 1 + \frac{h_n}{a_e} , \qquad H_{n+1} = 1 + \frac{h_{n+1}}{a_e} .$$

and a_e is the radius of the earth. E_n is the elevation angle of the ray path at the point at which it enters the nth layer. For the first layer, E_1 is the antenna elevation angle and the succeeding values of E_n are given by

$$E_n = \cos^{-1} \left[\frac{N_{n-1}}{N_n} \cos (E_{n-1}) \right]$$

where N_n is the index of refraction at the nth altitude.

The integral is then approximated using the trapezoidal rule

$$A(\nu, E) = \sum_{n=1}^{110} \left[\frac{\gamma_{n+1}(\nu) + \gamma_n(\nu)}{2} \right] (l_n) ,$$

where the subscript n denotes the value computed for the nth altitude. Similar calculations that do not allow for the bending of the ray path show that the attenuation is essentially the same for a given antenna elevation angle and that the only effect of refraction is to change the angle required for a given source.

The final results of the calculations giving the total attenuation due to atmospheric oxygen and water vapor are shown in Figs. 9 and 10 as a function of frequency for various antenna elevation angles and as a function of elevation for various frequencies in Fig. 11. The effect of the altitude dependence has sharpened the peaks and has produced a steep increase in the total attenuation below 10 degrees elevation. The plot in Fig. 10 shows on a linear scale the frequency and elevation dependence of total attenuation (less than 20 dB) and emphasizes the extremely steep frequency dependence near the oxygen resonances.

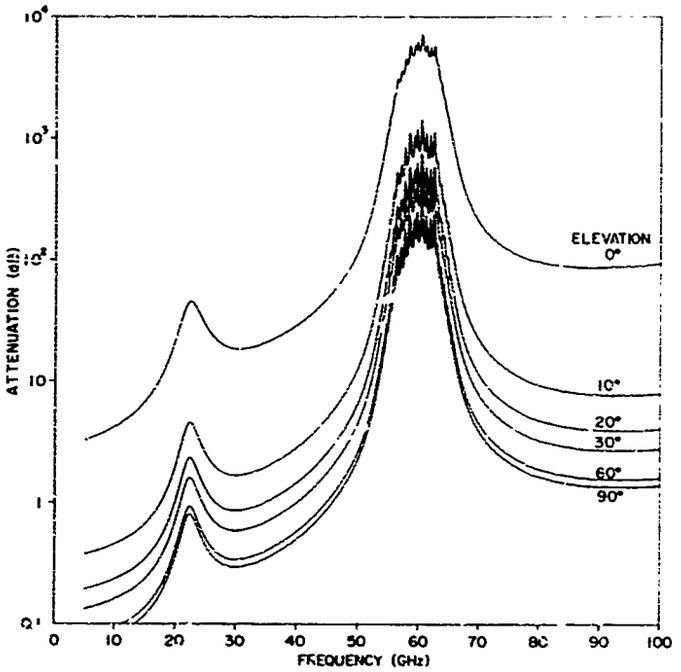

Fig. 9 - Total absorption vs frequency for paths through the atmosphere at various antenna elevation angles (ρ_0 = 7.5 g/m^3)

ATTENUATION BY RAINFALL

The attenuation due to rainfall is treated separately since the distribution of rain along the propagation path is generally unknown and unpredictable, making the results of rain attenuation calculations quite qualitative.

The theoretical treatment of rainfall attenuation is an exercise in classical electromagnetic theory. The general solutions to the wave equation in expansions of spherical functions are known. An incident plane wave, a scattered wave, and a transmitted wave are expressed in the spherical functions, and the coefficients of the expanded solutions

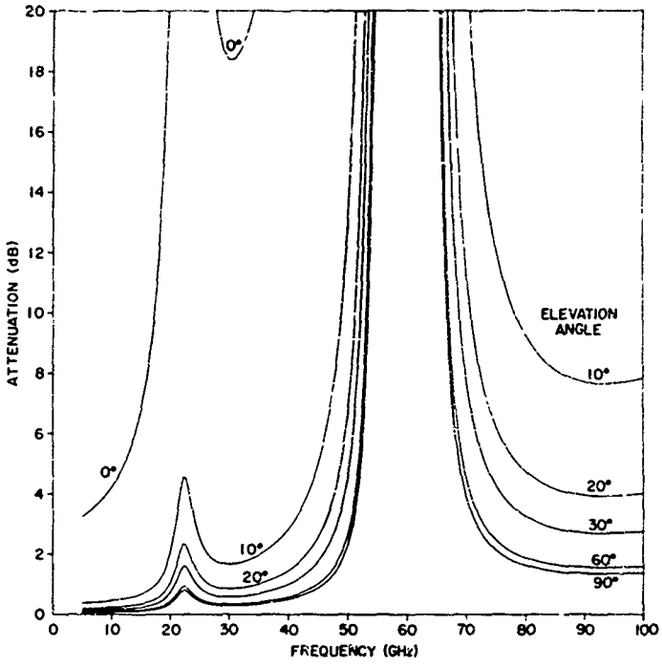

Fig. 10 - Total absorption vs frequency for paths through the atmosphere at various antenna elevation angles (ρ_0 = 7.5 g/m^3)

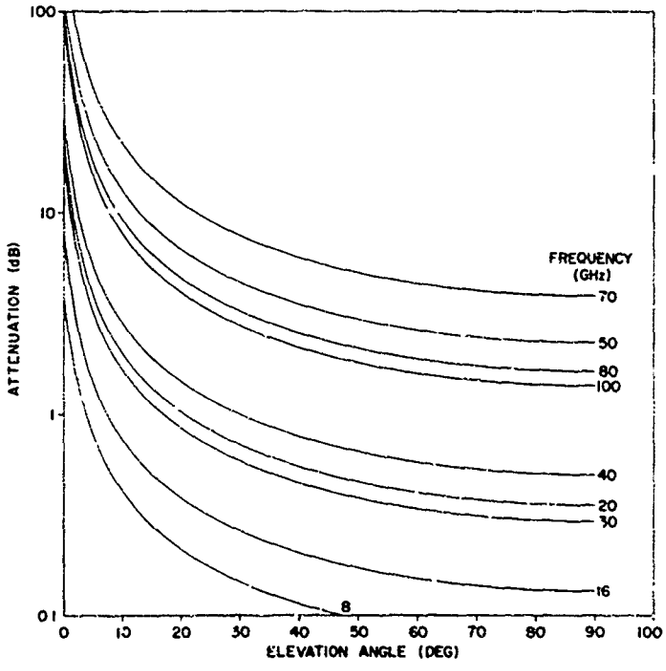

Fig. 11 - Total absorption vs antenna elevation angle for paths through the atmosphere at various frequencies (ρ_0 = 7.5 g/m^3)

are fitted to the boundary conditions at the surface of a spherical raindrop. The attenuation due to a single raindrop is obtained by comparing the absorbed and scattered energies with the incident energy.

The total attenuation due to the rainfall is then related to the rainfall rate using an empirically based model of the drop size vs number distribution as a function of rain rate by summing the attenuation due to the various size drops, neglecting the effect of multiple scattering.

The attenuation at frequencies from 4 to 100 GHz has been most recently treated by Oguchi (25,26) and has been reviewed with reference to the experimental evidence by Medhurst (27) and Crane (28). These papers also contain the earlier background references, detailed discussions of the theoretical solutions, and choice of drop size vs number vs rate distributions.

In attempting to estimate the actual effect of rainfall on propagation along paths through the atmosphere, the greatest difficulty is not in computing the magnitude of the attenuation once the characteristics of the rain are known, but in predicting these characteristics. In examining the attenuation observed during a given storm, the discrepancy between the measured and expected values will in greater part be due to departures of the rate and rate vs drop size distributions from the average and to the vagaries of the spatial distribution models in both altitude and range. The results of Oguchi's calculations are in good agreement with results of experiments in which the various rain parameters are known, and these results may be used without adding significantly to the error inherent in the assumption of models for rainfall distribution. Curves of attenuation vs frequency and rate interpolated from Oguchi's tabulated numerical results are given in Figs. 12 and 13.

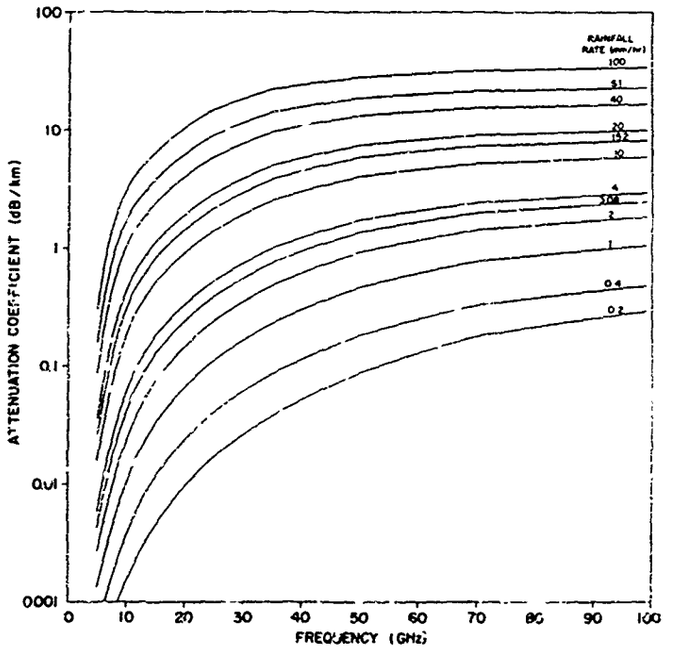

Fig. 12 - Theoretical rainfall attenuation vs frequency for various rain rates

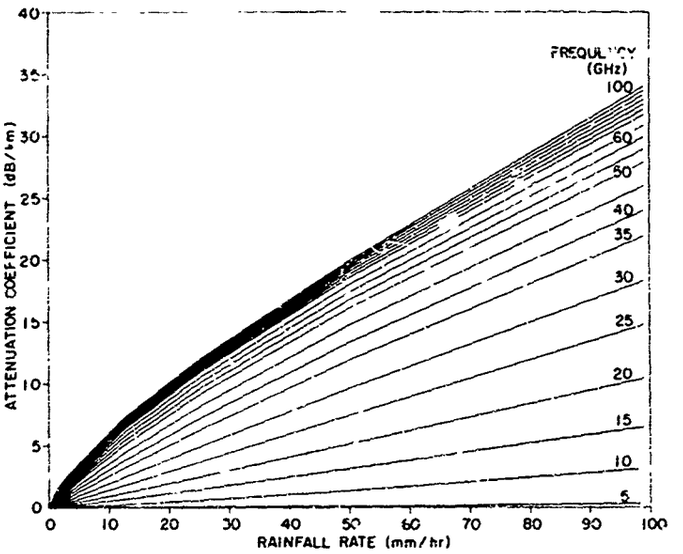

Fig. 13 - Theoretical rainfall attenuation vs rain rate for various frequencies

To discuss rainfall attenuation on a general basis without reference to a particular storm, it is necessary to use a statistical approach. A meaningful sampling of typical rainfall effects may be obtained by considering values of rainfall rates which will be exceeded 1, 0.1, and 0.01 percent of the time corresponding to light, moderate, and heavy rain.

Statistical studies of rain rate as a function of the total time a specific rate was exceeded over the time period of a year are available for various locations. The survey papers of Weible and Dressel (29) and Medhurst (27) contain lists of references for this and other types of studies that will be referred to here.

The results of Bussey (30) for Washington, D.C., give the instantaneous rain rate as a function of the total number of hours per year during which the rate is exceeded. The rate exceeded 87.6 hours per year or 1 percent of the time is 3.05 mm/hr; 15.2 mm/hr is exceeded 0.1 percent of the time; and 61.0 mm/hr 0.01 percent of the time.

Although it is known that light rains tend to fall over wide areas simultaneously while heavy rains are generally due to intense, highly localized storms, studies giving the relative rates as a function of the ground range from the observer at a given instant are not available. Rather, the observed quantities are given in terms of averages over time or over collecting area. Such averages necessarily include the effects of storm translation and are difficult to interpret precisely in terms of momentary distributions. Radar studies of individual storms (31) have suggested that a parabolic distribution is a fair approximation of that observed:

$$R_r(r) = 1 - \left[\frac{r}{a}\right]^2, \quad \text{for } r \leq a$$

$$R_r(r) = 0, \quad \text{for } r > a,$$

where $R_r(r)$ is the rain rate at ground distance r from center, relative to the rate at the center, and a is the radius of the storm (km).

The dependence of the rate on altitude based on model distributions of the various parameters, is given by Valley (32). Valley's curves can be fitted for computational purposes by the function

$$R_h(h) = (1.044) \exp[-0.173(h + 1)^2] ,$$

where $R_h(h)$ is rate at altitude h (km) relative to rate at ground.

In the absence of meaningful statistical studies of the instantaneous rainfall distributions, the following approximate models will be assumed:

Model No..	Time Exceeded (%)	Peak Rate (mm/hr)	Storm Radius a (km)
1	1.0	3.05	50
2	0.1	15.2	20
3	0.01	61.0	10

The cross sections of these model storms are shown in Fig. 14a, b, and c. To illustrate the coarseness of the models, the cross section of a real thunderstorm is reproduced in Fig. 14d.

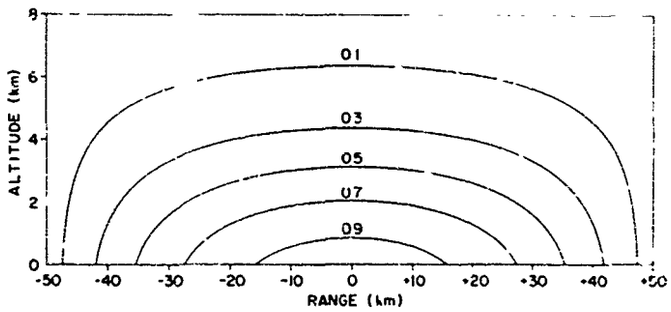

a. Model 1: a = 50 km

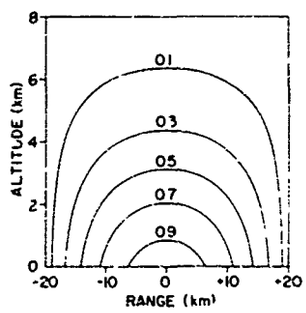

b. Model 2: a = 20 km

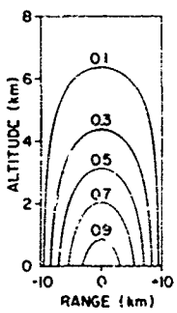

c. Model 3: a = 10 km

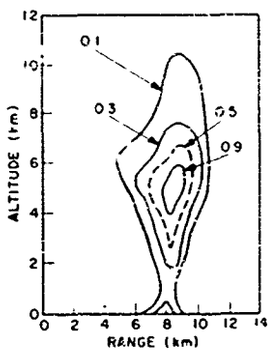

d. Real thunderstorm

Fig. 14 - Model rainstorms and a real thunderstorm, showing contours of relative rain rate

Since it is not possible to consider possible preferred azimuthal directions without prior knowledge of the synoptic conditions at a given site, it will be further assumed, as a coarse average over all directions, that the storm is centered on the site.

The range and altitude distributions may be combined to give an effective path length through the storm as a function of elevation angle E. The effective path length is

$$P(E) = \int_0^{\infty} R_r(l \cos E)\, R_h(l \sin E)\, dl ,$$

the distance through an equivalent storm of constant unit rain rate throughout, having the same total attenuation as the model storm. The use of such an effective path length assumes that the attenuation coefficient has a nearly linear dependence on rain rate. The approximate attenuation contributed by the rainfall can be obtained by multiplying this length by the attenuation coefficient corresponding to the local rain rate and the operating frequency;

$$A_{rain}(f, E, R_0) = \gamma_{rain}(f, R_0)\, P(E) ,$$

where

A_{rain} = attenuation due to rain (dB),

γ_{rain} = attenuation coefficient (dB/km), and

R_0 = local rain rate (mm/hr).

Figure 15 shows the effective path length as a function of elevation angle for storms of various radii based on the above models.

The rainfall attenuations computed in this way using the rough models should indicate at least the order of magnitude of the effect likely to be encountered. The attenuation values for the three model storms are added to the absorption due to oxygen and

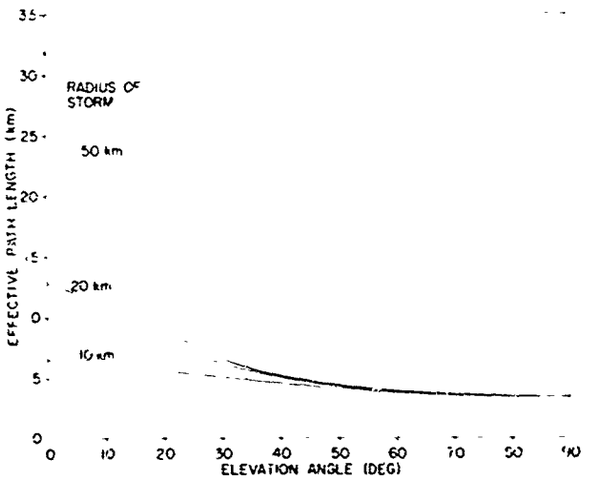

Fig. 15 - Effective path length vs elevation for model storms

water vapor and displayed as total attenuation in Figs. 16 through 18. It is clear that the rainfall attenuation is dominant at the higher frequencies for any but the lightest rain storm.

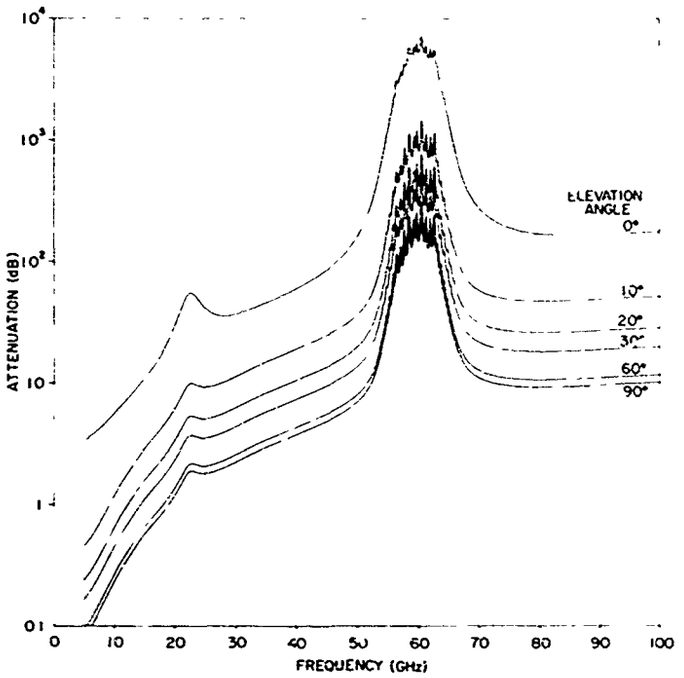

Fig. 16 - Total attenuation, Model Storm 1

CONCLUSION

The values of absorption coefficients used here are computed in detail from the theory as tempered by the available empirical evidence. They represent as accurately as possible the effect of atmospheric oxygen and water vapor on microwave radiation.

The values of total path attenuation, however, also depend on artificial models for the distribution of the atmospheric constituents, and the results must be viewed as representative of values likely to be encountered but not necessarily precise under all conditions.

The results obtained for the rainfall attenuation are intended only as a qualitative indication of the effect to be expected. Serious attempts to predict the rain losses must rest on meaningful statistical studies of instantaneous rainfall distributions at the site of interest. Experimental evidence is limited, and determination of the actual attenuation occurring along atmospheric paths at elevation angles other than zero must be made to refine the computed results and to determine the spread of values under a range of operating conditions.

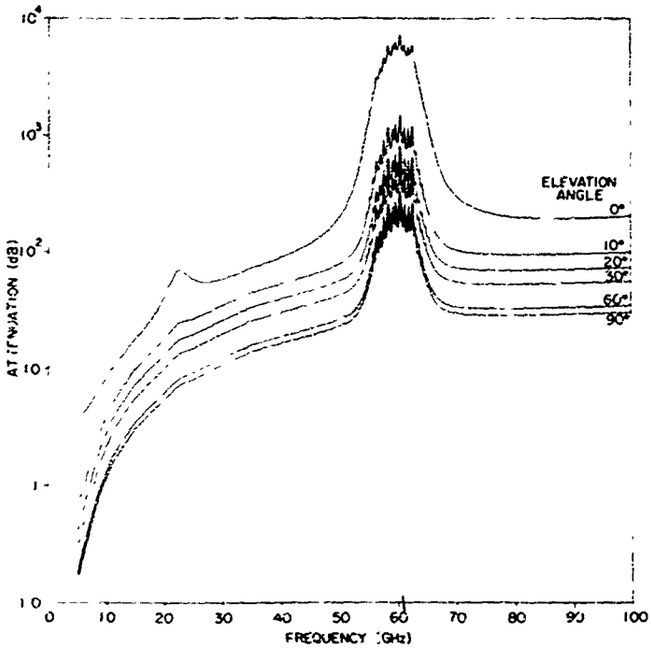

Fig. 17 - Total attenuation, Model Storm 2

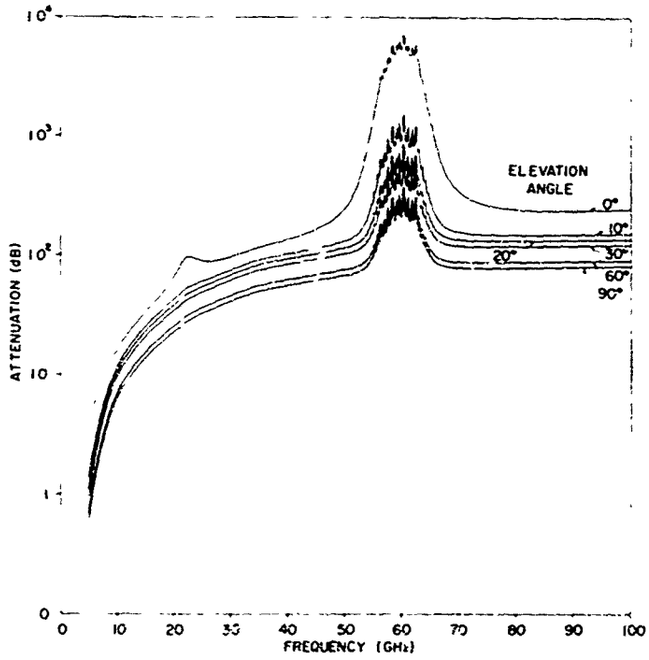

Fig. 18 - Total attenuation, Model Storm 3

SYMBOLS (in order of appearance)

f_j	Fraction of molecules in jth energy state
α	Absorption coefficient
ν	Frequency of radiation
N	Number of molecules per unit volume
μ_{ij}	Quantum mechanical matrix element connecting ith and jth molecular energy states
f_i	Fraction of molecules in energy state i
ν_{ij}	Resonant frequency of absorption line corresponding to the transition from state i to state j
$S(\nu_{ij}, \nu)$	Line shape function
K	Rotational quantum number
J	Total angular momentum quantum number
μ_0	The Bohr magneton
$\mu_{K\pm}$	Matrix element corresponding to transitions $K \rightarrow K+1 (+)$ and $K-1 \rightarrow K (-)$
(w.f.)	Statistical weight factor
E_i	Energy of ith state
k	Boltzmann's constant
T	Absolute temperature
Z	Partition function
$f_v(n)$	Fraction of states in vibrational state defined by principle quantum number n
$f_r(J, K, M)$	Fraction of states in rotational states defined a set of quantum numbers J, K, and M
M	Quantum number for the projection of J on the molecular axis
e	Base of natural logarithms
B	A constant
h	Planck constant
P_{O_2}	Partial pressure of O_2

P Total pressure

γ_0 Constant adjusted in this work to fit the theoretical expression for the absorption coefficient to experimental values at pressure P_0, temperature T_0

ν_{K^+} Resonant frequency corresponding to allowed transitions $K \rightarrow K+1(+)$ and $K-1 \rightarrow K(-)$

x Dummy parameter

ν_0 Resonant frequency of water vapor absorption

ρ Water vapor density

ρ_0 Water vapor density at P_0, T_0

η_0' Experimental constant fitted to resonant water vapor absorption

E_0 Energy of lower state of water vapor resonance transition at 22.254 GHz

$\Delta\nu$ Line breadth factor

τ Mean time between molecular collisions

σ Collision cross section

F Intermolecular force

r Distance between molecules

n Exponent of intermolecular force law

$(\Delta\nu)_0$ Measured line breadth at P_0, T_0

x Exponent of temperature dependence of line breadth at constant pressure

atm Atmosphere (pressure)

ζ Constant of suggested pressure dependence of resonant frequencies of absorption lines

ζ_{O_2} Value of ζ for O_2

ζ_{H_2O} Value of ζ for H_2O

η_{res}' Experimental constant fitted to residual water vapor absorption

E Elevation angle of antenna

$A(\nu, E)$ Total attenuation at frequency ν and elevation angle E

l Distance along propagation path

l_n Distance along propagation path through the nth layer

°F Degrees Fahrenheit

°K Degrees Kelvin

H_n $1 + h_n/a_e$

h_n Height of nth layer

a_e Radius of earth

γ_n Total absorption coefficient at height h_n

E_n Local elevation angle at the nth layer

N_n Index of refraction at height h_n

$R_r(r)$ Relative rainfall rate at distance r from center of storm

$R_h(h)$ Relative rainfall rate at height h

a Radius of model rain storm

P_e Effective path length

$\gamma_{rain}(\nu, R_0)$ Rainfall attenuation coefficient corresponding to frequency ν, rainfall rate R_0

R_0 Local rain rate (mm/hr)

A_{rain} Attenuation due to rain (dB)

ACKNOWLEDGMENTS

Figures 2 through 18 were produced by a Gerber Automatic Drafting Machine operated by Mr. Stanley Kozloski of the NRL Engineering Services Division. Computer subroutines required to produce the punched paper tape for the drafting machine were written and furnished by Mr. A. T. McClinton of the NRL Atmosphere and Astrophysics Division.

Mr. J. P. Leiphart has reviewed this report and made many helpful suggestions.

REFERENCES

1. Mizushima, M., and Hill, R.M., "Microwave Spectrum of Oxygen," Phys. Rev. 93:745 (Feb. 1954)

2. Townes, C.H., and Schawlow, A.L., "Microwave Spectroscopy," New York:McGraw-Hill, 1955

3. Schlapp, R., "Fine Structure in the $^3\Sigma$ Ground State of Oxygen Molecule, and the Rotational Intensity Distribution in Atmospheric Oxygen Band," Phys. Rev. 51:343 (Mar. 1937)

4. Van Vleck, J.H., "Absorption of Microwaves by Oxygen," Phys. Rev. 71:413 (Apr. 1947)

5. Van Vleck, J.H., "The Absorption of Microwaves by Uncondensed Water Vapor," Phys. Rev. 71:425 (Apr. 1947)

6. Burkhalter, J.H., et al., "Fine Structure of Microwave Absorption Spectrum of Oxygen," Phys. Rev. 79:651 (Aug. 1950)

7. King, G.W., et al., "Expected Microwave Absorption Coefficient of Water and Related Molecules," Phys. Rev. 71:433 (Apr. 1947)

8. Van Vleck, J.H., and Weisskopf, V.F., "Shape of Collision-Broadened Lines," Rev. Mod. Phys. 17:227 (Jul. 1945)

9. Anderson, R.S., Smith, W.V., and Gordy, W., "Line Breadths of Microwave Spectrum of Oxygen," Phys. Rev. 87:561 (Aug. 1952)

10. Gokhale, B.V., and Strandberg, M.W.P., "Line Breadths in 5 mm Microwave Absorption of Oxygen," Phys. Rev. 84:844 (Nov. 1963)

11. Artman, J.O., and Gordon, H.P., "Absorption of Microwaves by Oxygen in Millimeter Wavelength Region," Phys. Rev. 96:1237 (Dec. 1954)

12. Beringer, R., "Absorption of One Half Centimeter Electromagnetic Waves in Oxygen," Phys. Rev. 70:53 (May 1946)

13. Lamont, H.R.L., "Atmospheric Absorption of Microwaves," Phys. Rev. 71:353 (Dec. 1948)

14. Lamont, H.R.L., "Atmospheric Absorption Millimeter Waves," Proc. Phys. Soc. 61:562 (Dec. 1948)

15. Crawford, et al., "Millimeter Wave Research," Final Report 24261-15, Bell Telephone Laboratories, Contract Nonr-687(00), Oct. 1955

16. Strandberg, M.W.P., Meng, C.Y., and Ingersoll, J.G., "Microwave Absorption Spectrum of Oxygen," Phys. Rev. 75:1524 (May 1949)

17. Iannuzzi, M., and Minnaja, N., "Pressure Effect on Microwave Absorption of Oxygen," Nuovo Cimento 30:997 (Nov. 1963)

18. Tinkham, M., and Strandberg, M.W.P., "Line Breadths in the Microwave Magnetic Resonance Spectrum of Oxygen," Phys. Rev. 99:537 (Jul. 1955)

19. Beringer, R., and Castle, J.G., Jr., "Microwave Magnetic Resonance Spectrum of Oxygen," Phys. Rev. 81:82 (Jan. 1951)

20. Becker, G.E., and Autler, S.H., "Water Vapor Absorption of Electromagnetic Radiation in Centimeter Wavelength Range," Phys. Rev. 70:300 (Sept. 1946)

21. Benedict, W.S., and Kaplan, L.D., "Calculation of Line Widths in H_2O - N_2 Collisions," J. Chem. P. 30:388 (Feb. 1959)

22. Schulkin, M., "Determination of Microwave Atmospheric Absorption Using Extraterrestrial Sources," NRL Report 3843 (Oct. 1951)

23. U.S.A.F., "Handbook of Geophysics," Rev. ed., New York:MacMillan, 1960

24. Blake, B.L., "Curves of Atmospheric-Absorption Loss for Use in Radar Range Calculations," NRL Report 5601, Mar. 1961

25. Oguchi, T., "Attenuation of Electromagnetic Waves due to Rain with Distorted Raindrops," J. of Radio Res. Lab. (Japan) 7:467 (Sept. 1960)

26. Oguchi, T., "Attenuation of Electromagnetic Waves due to Rain with Distorted Raindrops (II)," J. of Radio Res. Lab. (Japan) 11:19 (Sept. 1964)

27. Medhurst, R.G., "Rainfall Attenuation of Centimeter Waves: Comparison of Theory and Measurement," IEEE Trans. AP 13:550, Jul. 1965

28. Crane, R.K., "Microwave Scattering Parameters for New England Rain," M.I.T. Lincoln Laboratory Technical Report 426 (ESD-TR-66-447), Oct. 1966

29. Weibel, G.E., and Dressel, N.O., "Propagation Studies in Millimeter Wave Link Systems," IEEE Proc. 55(No. 4):497 (Apr. 1967)

30. Bussey, H.E., "Microwave Attenuation Statistics Estimated from Rainfall and Water Vapor Statistics," IRE Proc. 38:781 (Jul. 1950)

31. Atlas, D., and Banks, H.C., "The Interpretation of Microwave Reflections from Rainfall," J. Meteorol. 8:271, Oct. 1951

32. Valley, S.E., ed., "Handbook of Geophysics and Space Environments," Ch. 5, "Precipitation, Clouds, and Aerosols," New York:McGraw-Hill, 1965

Security Classification

DOCUMENT CONTROL DATA - R & D

(Security classification of title, body of abstract and indexing annotation must be entered when the overall report is classified)

1 ORIGINATING ACTIVITY (Corporate author) Naval Research Laboratory Washington, D.C. 20390	2a. REPORT SECURITY CLASSIFICATION UNCLASSIFIED 2b. GROUP

3 REPORT TITLE

ATTENUATION OF MICROWAVE RADIATION FOR PATHS THROUGH THE ATMOSPHERE

4 DESCRIPTIVE NOTES (Type of report and inclusive dates) An interim report on these problems; work on other phases is continuing.

5 AUTHOR(S) (First name, middle initial, last name)

R. A. LeFande

6 REPORT DATE November 29, 1968	7a. TOTAL NO OF PAGES 32	7b NO OF REFS 32
8a CONTRACT OR GRANT NO NRL Problems R01-34 and R01-36 b. PROJECT NO RF 14-222-41-4353; XF 019-02-04-11648 c d	9a. ORIGINATOR'S REPORT NUMBER(S) NRL Report 6766 9b. OTHER REPORT NO(S) (Any other numbers that may be assigned this report)	

10 DISTRIBUTION STATEMENT

This document has been approved for public release and sale; its distribution is unlimited.

11 SUPPLEMENTARY NOTES	12 SPONSORING MILITARY ACTIVITY Dept. of the Navy (Office of Naval Research and Naval Electronics Systems Command), Washington, D.C. 20360

13 ABSTRACT

Microwave radiation is absorbed by atmospheric oxygen and water vapor and is absorbed and scattered by rainfall. This report provides values of these losses in the frequency decade from 10 to 100 GHz for paths through the atmosphere at elevation angles from 0 to 90 degrees.

The theoretical expressions for oxygen absorption are assembled in explicit form. The resonant frequencies are taken from published low-pressure measurements, and the entire absorption profile is fitted to published intermediate and atmospheric pressure results, with a constant of proportionality and the absorption resonance line width used as fitting parameters. The absorption line breadth is found to deviate from the accepted linear pressure dependence, increasing approximately as the square root of pressure for pressures above one-half atmospheric.

The results of similar analyses of water vapor absorption are assembled and combined with the results of oxygen absorption analyses to obtain the complete absorption coefficients as a function of the atmospheric parameters.

The total attenuation due to absorption in the clear atmosphere is computed for a model atmosphere with various water vapor concentrations. Results are provided in graphical form, giving attenuation as a function of frequency and elevation angle.

(over)

DD FORM 1 NOV 65 1473 (PAGE 1)

S/N 0101-807-6801

Security Classification

Security Classification

14 KEY WORDS	LINK A		LINK B		LINK C	
	ROLE	WT	ROLE	WT	ROLE	WT
Attenuation						
Microwave radiation						
Atmosphere						
Absorption						
Oxygen						
Water vapor						
Absorption line shape						
Rainfall attenuation						
Model rain storms						
Line breadth						
Propagation						

The prediction of rainfall attenuation is severely limited by the absence of meaningful statistics on rain rate and storm structure. Rough estimates for rain attenuation are made for crude model storms which occur for 1, 0.1, and 0.01 percent of the time. Total values of the attenuation for the model storms and the atmospheric absorption are provided.

DD FORM 1 NOV 68 1473 (BACK)
(PAGE 2)

Security Classification

NRL Report 6766
Change 1
May 27, 1969

1. On p. 2, nine lines up from the bottom, the word "processing" should read "precessing."

2. On pages 14 and 15, the caption for Fig. 6 belongs to Fig. 8, and vice versa.

NAVAL RESEARCH LABORATORY
WASHINGTON, D.C.